



OPEN

SUBJECT AREAS:
SURFACE PATTERNING
SCANNING ELECTRON
MICROSCOPYReceived
16 October 2013Accepted
25 November 2013Published
16 January 2014Correspondence and
requests for materials
should be addressed to
S.K. (kuwabata@
chem.eng.osaka-u.ac.
ip)

Three-dimensional micro/nano-scale structure fabricated by combination of non-volatile polymerizable RTIL and FIB irradiation

Susumu Kuwabata¹, Hiro Minamimoto¹, Kosuke Inoue¹, Akihito Imanishi², Ken Hosoya³, Hiroshi Uyama¹, Tsukasa Torimoto⁴, Tetsuya Tsuda¹ & Shu Seki¹

¹Department of Applied Chemistry, Graduate School of Engineering, Osaka University, 2-1 Yamada-oka, Suita, Osaka 565-0871, Japan, ²Department of Chemistry, Graduate School of Engineering Science, Osaka University, 1-3 Machikaneyama, Toyonaka, Osaka 560-8531, Japan, ³Graduate School of Life and Environmental Science, Kyoto Prefectural University, 1-5 Hangi-cho, Shimogamo, Sakyo-ku, Kyoto 606-8522, Japan, ⁴Department of Crystalline Materials Science, Graduate School of Engineering, Nagoya University, Chikusa-ku, Nagoya, Aichi 464-8603, Japan.

Room-temperature ionic liquid (RTIL) has been widely investigated as a nonvolatile solvent as well as a unique liquid material because of its interesting features, e.g., negligible vapor pressure and high thermal stability. Here we report that a non-volatile polymerizable RTIL is a useful starting material for the fabrication of micro/nano-scale polymer structures with a focused-ion-beam (FIB) system operated under high-vacuum condition. Gallium-ion beam irradiation to the polymerizable 1-allyl-3-ethylimidazolium bis((trifluoromethane)sulfonyl)amide RTIL layer spread on a Si wafer induced a polymerization reaction without difficulty. What is interesting to note is that we have succeeded in provoking the polymerization reaction anywhere on the Si wafer substrate by using FIB irradiation with a raster scanning mode. By this finding, two- and three-dimensional micro/nano-scale polymer structure fabrications were possible at the resolution of 500,000 dpi. Even intricate three-dimensional micro/nano-figures with overhang and hollow moieties could be constructed at the resolution of approximately 100 nm.

Focused-ion-beam (FIB) irradiation is a powerful approach for carving three-dimensional (3D) materials and for drawing two-dimensional (2D) patterns by sputtering¹⁻⁷. Another fascinating feature is the ability to make up micro- or nanometer size 3D figures by the combination of FIB irradiation and chemical vapor deposition (CVD). This technique known as a FIB-chemical vapor deposition (FIB-CVD) technique needs a reactive gas, such as phenanthrene, as a precursor to produce 3D figures. The gas directly introduced by a special device into a FIB equipment is converted into a solid deposit on a substrate by a FIB irradiation⁸. By the approach with a common raster scanning mode, simple standing wire and tube figures can be constructed. However, the fabrication of intricate 3D figures, e.g., overhang and hollow parts, requires a specialized FIB-CVD system, which enables FIB irradiation with a vector mode. Fundamental operating principles of this technique have been developed by Matsui et al^{9,10}. The system is designed for providing phenanthrene gas after searching an appropriate voxel, which must be adjacent to a voxel already occupied by a deposit, to produce the 3D figures, because the ion beam irradiation in midair cannot make a contribution to the production as a matter of course. Unfortunately, at this moment, this is not a common technique to fabricate 3D structures.

Liquids such as water and organic solvents are, in general, considered as inappropriate substances for being handled under vacuum condition. Introduction of any type of liquids is therefore strictly prohibited in all instruments, which require vacuum condition, including sputtering equipment, X-ray photoelectron spectroscopy, electron microscope, and FIB irradiation instrument. However, the incompatibility between the liquid substances and such instruments is now becoming a thing of the past with the advent of room-temperature ionic liquid (RTIL). RTIL is a type of organic salt with a low melting point below room temperature. RTIL's interesting features, which include negligible vapor pressure, flame retardation property, relatively-high ionic conductivity, are opening new various areas of investigations¹¹⁻¹⁸. Of them, RTIL-based vacuum technology seems to be a promising field¹⁹⁻²². Also, we have contributed the development of the field and created several RTIL-based

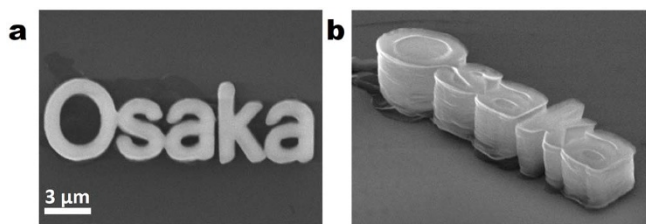


Figure 1 | SEM images of three-dimensional polymer microstructures. The patterned structures were deposited in a thin [AllylEtIm][Tf₂N] layer on a Si substrate using FIB irradiation with a raster scanning mode. (a) Polymers having “Osaka” characters with a high resolution. (b) Oblique angle image of Fig. 1a shows that these polymer patterns have 3D structures. This polymer patterns were obtained with the ion dose of 300×10^{15} ions cm^{-2} and the number of scanning of 100 times.

vacuum technologies. We found that magnetron sputtering onto RTIL yields a wide variety of metal and alloy nanoparticles without any stabilizing agent^{23,24} and that RTIL itself can be observed by a scanning electron microscope without accumulation of electrostatic charge at the surface of RTIL²⁵. The latter is applicable to scanning electron microscope (SEM) and transmission electron microscope (TEM) observations of hydrated specimens pretreated with RTIL and to in situ SEM observation of chemical reactions in RTIL^{26–29}.

It is well-known that chemical reactions are induced in varying degrees when some sort of specimen is irradiated with a FIB and an electron beam, which are ionizing radiations^{30,31}. If the reaction can be controlled at micro/nano-scale in RTIL, fabrication of 3D micro/nanostructure is expected with ease like a 3D printing technique. In this study, we attempted to establish the method that can three-dimensionally control the polymerization reaction in a polymerizable 1-allyl-3-ethylimidazolium bis((trifluoromethane)sulfonyl)amide ([AllylEtIm][Tf₂N]) RTIL thin layer onto a Si wafer by using a common FIB technique with a raster scan mode, not need a specialized FIB system. The formation process of the 3D structures produced by the RTIL-based FIB irradiation method was also examined.

Results

Polymer pattern deposits prepared by RTIL-based FIB irradiation method. In each FIB drawing experiment, bitmapped images were designed at a display frame of 800×800 pixels in advance. FIB drawing was carried out in a raster scanning mode at a $40 \mu\text{m} \times 40 \mu\text{m}$ area based on the designed image. The detailed experimental condition is described in “Method” section. Our first FIB drawing was characters of “Osaka” onto an [AllylEtIm][Tf₂N] RTIL layer spread on a Si wafer ([AllylEtIm][Tf₂N]/Si). The resulting SEM image of the top view is shown in Fig. 1a, indicating that the desired polymer pattern was successfully produced as a result of the local polymerization reaction of the [AllylEtIm][Tf₂N] induced by the FIB irradiation. Surprisingly, the SEM image from different angles revealed that the characters are 3D “Osaka” as shown in Fig. 1b and that the “Osaka” is formed by a layer-by-layer assembly.

To elucidate how the pattern grew in the vertical direction, FIB drawings of square frame were conducted at different dosages. Figure 2a shows a SEM image of the structures obtained on a [AllylEtIm][Tf₂N]/Si at different ion doses, D , of 100, 200, 300, 400, and 500×10^{15} ions cm^{-2} . In this investigation, the beam current, I_B , and the dwell time, t_{dw} , were 48 pA and 250 μs , respectively. The number of pixels, n_{pix} , was 4.0×10^{10} pixels cm^{-2} . The number of raster scan, N , during the FIB drawing experiment is an important parameter for fabricating 3D figures, and the N can be estimated by the following equation:

$$N = \frac{D}{(I_B/e) \times t_{\text{dw}} \times n_{\text{pix}}} \quad (1)$$

where e is the elementary charge. Therefore, when the D is 100, 200, 300, 400, and 500×10^{15} ions cm^{-2} , the N is 33, 66, 100, 133, and 166 times, respectively. The increase in the N directly related to the increase in the height of the 3D figures, H . Figure 2b summarizes the relationship between the H and the N values or the D values. The plotted H values were calculated by:

$$H = \frac{h}{\sin 75^\circ} \quad (2)$$

where h is the value of height obtained from SEM image shown in Fig. 2a and 75° is the tilt angle for the SEM observation. The H was

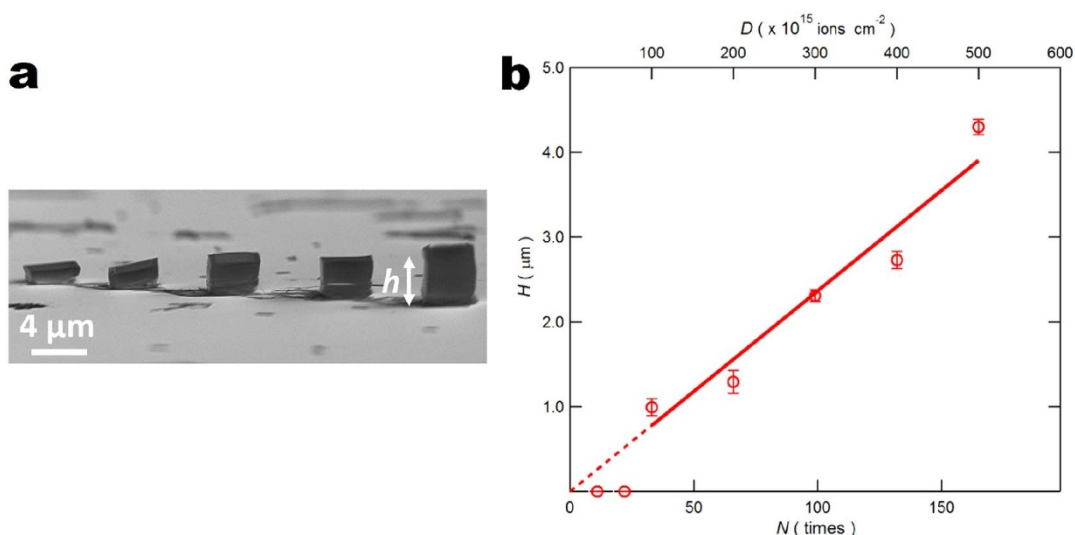


Figure 2 | Three-dimensional square frame polymer structures prepared under different ion dose conditions. (a) SEM image of square frame structures deposited in a thin [AllylEtIm][Tf₂N] layer on a Si substrate prepared by RTIL-based FIB irradiation method with a raster scanning mode. The image was taken at a tilt angle of 75° . The ion, D , doses were 100×10^{15} , 200×10^{15} , 300×10^{15} , 400×10^{15} , and 500×10^{15} ions cm^{-2} from the left to right structure, and then the numbers of scanning estimated from the ion doses, N , were 33, 66, 100, 133, and 166 times. The height of the structures increased with the increase in the N , i.e., with the increase in the D . (b) Relationship between the heights of the polymer structures and the N or the D . The polymer structure could not be obtained with the N less than 33 times.

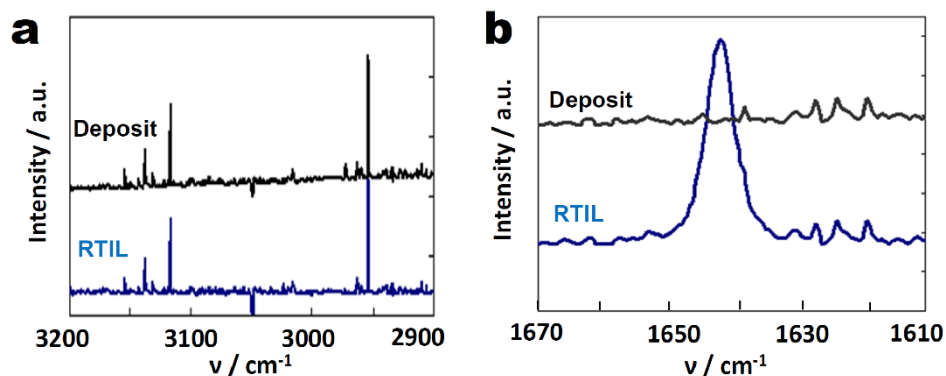


Figure 3 | Micro-Raman spectra of neat [AllylEtIm][Tf₂N] RTIL and the resulting polymer structure. The wavenumber regions were (a) between 2900 and 3200 cm⁻¹ and (b) between 1610 and 1670 cm⁻¹. The spectra obtained at higher wavenumber suggest that imidazolium cation exists in both the neat RTIL and the polymer deposit. The disappearance of the band at 1645 cm⁻¹ indicates that the allyl group on the [AllylEtIm]⁺ is involved in the polymerization reaction.

approximately proportional to the N values if it was over 33 cycles; however, no figure was observed by SEM when the N was below 33 cycles. The minimum height of the 3D structure was ca. 1.0 μm . As described in the “Method” section, the RTIL was spread onto a Si wafer by a spin coater so as to obtain a uniform liquid layer with a thickness of ca. 1.0 μm . We expected the maximum height is dependent on the RTIL layer thickness, but it was not. The height continued to increase with the increase in the N , and the height apparently exceeded the RTIL layer thickness. For example, at the 166 cycles, the height became almost 4.3 μm . These results provided a clue to propose the mechanism of 3D pattern formation with our RTIL-based FIB irradiation method, as will be described later.

Chemical reactions in [AllylEtIm][Tf₂N] under FIB irradiation.

The deposit obtained by the FIB irradiation onto the [AllylEtIm][Tf₂N]/Si was characterized by a Raman microscope. Raman spectra of the [AllylEtIm][Tf₂N] and the obtained deposit contained some Raman bands in the wavenumber range between 2950–3150 cm⁻¹ because of the existence of the imidazolium ring³² (Fig. 3a). It suggests that the imidazolium cations remain in the deposit produced after the FIB irradiation. In the spectrum of the neat RTIL, the Raman band that is assignable to a stretching vibration of the double bond of the allyl group appeared at 1645 cm⁻¹; however, the band disappeared in the spectrum of the deposit (Fig. 3b). The absence of this band indicates that the polymerization reaction on the allyl group proceeded during the FIB irradiation. In fact, allyl group is known to be difficult to polymerize by a common radical polymerization method, since the allyl radical has a stable resonant structure. Successive radical polymerization reactions are not expected although oligomers are formed^{33,34}. The polymerization reaction observed in this investigation may be peculiar to the [AllylEtIm][Tf₂N] under the FIB irradiation as described below in detail.

Resolution of polymer deposit. The resolution of the polymer structure produced by the RTIL-based FIB irradiation method was examined through drawing a two-dimensional intricate picture. Figure 4a is a photograph of a famous Japanese picture titled “Beauty Looking Back” (“Mikaeri-bijin” in Japanese) used in this experiment. The original picture was drawn by one of a great Japanese artist, Moronobu Hishikawa, during the Edo period (1603–1868 A.D.). A bitmap file for drawing the FIB irradiation pattern was created by scanning a reproduction of the picture. The bitmap figure is depicted in Fig. 4b. As shown in Fig. 4c, we could draw a microscale “Beauty Looking Back” by the use of our approach. The resulting polymer structure accurately duplicates the bitmap file design. The resolution was approximately 100 nm according to the

magnified image of a design on a Kimono, a Japanese traditional dress. This nanoscale resolution is a great advantage of the RTIL-based FIB irradiation method because other microstructure fabrication methods do not achieve such resolution scale. For example, the resolution of FIB-CVD method is about 200 ~ 300 nm^{8,35,36}.

Fabrication of intricate three-dimensional figures. As mentioned in introduction, one of the fascinating features of FIB-CVD operated in a vector mode is the ability to produce intricate 3D figures with overhang and hollow parts. Our RTIL-based FIB irradiation method that is the combination of the polymerizable RTIL and the common FIB technique with a conventional raster scanning mode also enables to fabricate complicated 3D figures. These examples are shown in Fig. 5. A teacup-shape figure was formed by overdrawing different size circles (Fig. 5a). A bridge structure, as shown in Fig. 5b, was constructed by drawing two separate square frame patterns, followed by drawing another square frame pattern so as to bridge the

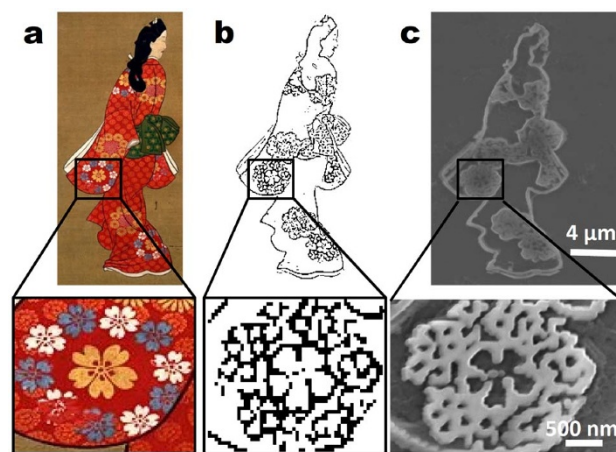


Figure 4 | Two-dimensional polymer structure prepared by RTIL-based FIB-irradiation method. (a) A famous Japanese picture titled, “Beauty Looking Back.” This picture was painted by a Japanese artist, Moronobu Hishikawa, in the Edo period. (b) Bitmap image of “Beauty Looking Back” created for the FIB drawing. (c) SEM image of a 2D polymer structure fabricated from the bitmap image. The enlarged view of the flower painted on the “Kimono” is shown under each picture. The irradiation conditions for fabrication of this structure were the ion dose of 100×10^{15} ions cm⁻² and the number of scanning of 33 times. The painting ‘Beauty Looking back’ is reprinted with permission from the Tokyo National Museum.

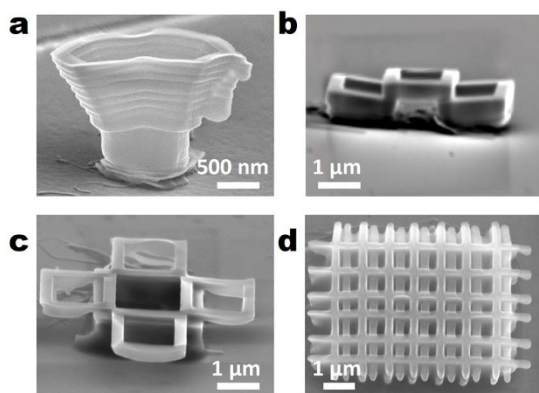


Figure 5 | Various three-dimensional polymer structures. (a) Teacup structure. The structure was achieved by stacking circle patterns in layers. (b) Bridge structure. The structure has a hollow construction. The two square frame structures were prepared first, and another square frame structure was drawn at the center so as to overlap the previously deposited two square figures. (c) A jack-in-a-box structure. The four upper square frame structures protrude from the base one. This result shows that overhang structures were formed without depending on the scanning directions. (d) Woodpile structure. This structure is known as one of the 3D photonic crystals. These structures were obtained by RTIL-based FIB irradiation method with a raster scanning mode.

previously prepared 3D patterns. Even like a jack-in-a-box structure shown in Fig. 5c could be fabricated. It was composed of five 3D square frame patterns; first of all one 3D square pattern was deposited as a base, and after that four slightly smaller 3D square frame patterns were separately drawn by the FIB in order to position one side of each smaller square on one of the four sides on the top of the base square. The figure with long hanging structures, which are technically impossible to prepare by a FIB sputtering method, was eventually prepared. The four overlapped structures were equally

formed at four sides on the top of the base square, indicating that the formation of the hanging structure occurs irrespective of the direction of the raster scanning. We have also succeeded in formation of a photonic crystal-like 3D network structure (woodpile structure) by the same approach (Fig. 5d).

Another complex structure was designed to find a clue about the formation mechanism of the 3D structures by the RTIL-based FIB irradiation method. This figure was prepared by deposition of a rectangular frame base, followed by drawing of two square frame patterns; one square frame was located adjacent to the base, and another was put its one side on one side of top of the base rectangle structure (Fig. 6a). Apparently the former pattern was directly deposited onto the Si wafer (Fig. 6b), whereas the latter was formed onto the base structure (Fig. 6c). The formation of the hanging structure suggests that the polymerization reaction occurs at the position higher than the previously prepared deposit because the latter frame pattern did not deposit on the Si substrate although the FIB drawing was initiated from left bottom as shown in Fig. 6a.

Discussion

As is well known, ion beam irradiation to polymer materials including polyethylene and polystyrene generates radicals that come from hydrocarbon backbones, and then cross-linkage reaction among the backbones proceeds^{37–40}. It is highly likely that similar cross-linkage reaction occurs among the [AllylEtIm]⁺ oligomers yielded during the FIB irradiation. As a result, rigid polymer derived from the [AllylEtIm][Tf₂N] would be obtained. In order to investigate other non-volatile polymerizable RTIL for the RTIL-based FIB irradiation method, we also carried out the same experiment using 1-vinyl-3-butylimidazolium bis((trifluoromethane)sulfonyl)amide ([VinylBuIm][Tf₂N]) that has an easily polymerizable vinyl group. Because polymerization rate for linear polymers without crosslinks of vinyl groups is much faster than the oligomerization of allyl groups^{33,34}, it was very difficult to control the polymerization reaction induced by the FIB irradiation. It is then likely that the reaction proceeded three-dimen-

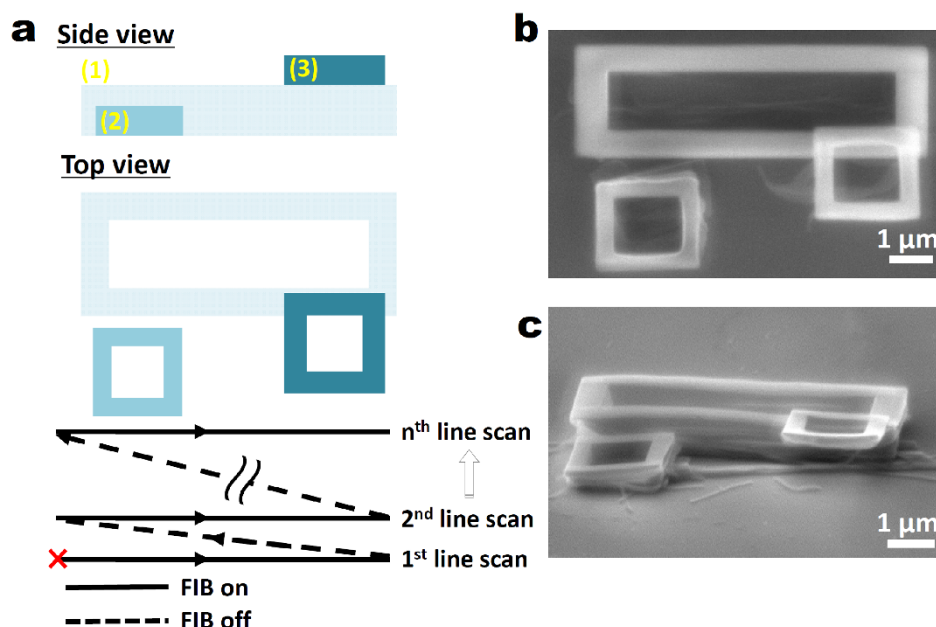


Figure 6 | Complicated three-dimensional polymer structures. (a) Drawing design for fabrication of the polymer patterns shown in Fig. 6b and c. First, the large rectangular frame structure (1) was drawn as a base. Second, the small square frame structure (2), which did not overlap the base polymer, was drawn at the left side of the base. Finally, another small square frame structure (3) was prepared on the base, but only one side of the small square overlapped on part of the base. The FIB irradiation with a raster scanning was initiated from the X. The direction was indicated by the arrows. (b) SEM image of polymer structures prepared by the design depicted in Fig. 6a. (c) Oblique angle image of Fig. 6b. This SEM image indicates the small square frame structure on the right side protrudes from the base, although another small square on the left side is on the substrate.

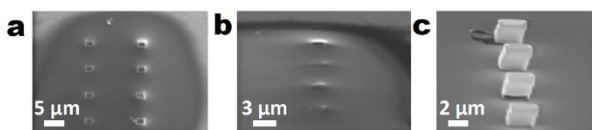


Figure 7 | SEM images of three-dimensional square frame structures covered with and without RTIL. (a) SEM image of several square structures before rinsing off the [AllylEtIm][Tf₂N] RTIL. (b) Another SEM image taken from a different angle. The meniscus derived from the surface tension was observed on the polymer patterns. All the structures were covered with the RTIL layer. (c) SEM image of Fig. 7b after rinsing the RTIL off using acetonitrile. The height of the structures exceeded the RTIL layer thickness of ca. 1 μm. The irradiation conditions for fabrication of this structure were the ion dose of 300×10^{15} ions cm⁻² and the number of scanning of 100 times.

sionally beyond the irradiated position. The resulting polymer structures on the [VinylBuIm][Tf₂N]/Si are shown in Fig. S1. Very thin square frame deposits were obtained, but unexpected irregular structures attributed to the uncontrolled polymerization reaction also appeared. We strongly believe that the RTIL with the allyl group is the most suitable for the RTIL-based FIB irradiation method at this time.

As described above, some 3D structures were produced over the RTIL film thickness (ca. 1 μm). It can be explained by the surface tension of the RTIL itself. Figure 7 indicates SEM images of the prepared square frame patterns before and after rinsing the unreacted [AllylEtIm][Tf₂N] off using acetonitrile. All the prepared patterns were designed to be ca. 2.0 μm high. Before rinsing, the deposited patterns were completely covered with the RTIL, due to the surface tension of the RTIL (Fig. 7a and b). But after rinsing, the square frame patterns exceeding the original RTIL layer thickness of ca. 1.0 μm appeared (Fig. 7c).

On the basis of several findings in this study, we proposed a plausible formation process for 3D polymer structures by the RTIL-based FIB irradiation method. As depicted in Fig. 8, at the initial stage, polymerization reaction of the [AllylEtIm][Tf₂N] proceeds by FIB irradiation at the surface of the RTIL layer, and polymer layer is formed in accordance with the design programmed in advance (Fig. 8a). When the FIB drawings are repeated, the polymer deposit

grows downward until it reaches the Si wafer (Fig. 8b and c). If the bottom of the polymer structure reaches the Si wafer, it physically adheres to the Si wafer. It is also possible that some chemical bondings via Si-OH contribute the adhesion. Once the structure is immobilized onto the Si wafer, subsequent FIB irradiation causes a further polymerization on the immobilized structure (Fig. 8d–f). Because RTIL exists on the top of the polymer structure owing to the surface tension with meniscus of the RTIL as described in the preceding paragraph, the height does not depend on the RTIL layer thickness. In some cases those were over 4 μm high. Therefore, the RTIL-based FIB method makes it possible to fabricate a wide variety of 3D micro- or nanostructures with hanging and bridging parts but not produce the polymer structure that is less than ca. 1 μm high as shown in Fig. 2 because the structure is not immobilized until it reaches the Si wafer surface. Monte Carlo simulation⁴¹ on the gallium-ion travel distance through the RTIL strongly supports our idea that the polymerization reaction occurs at the surface of RTIL. The detailed information on the simulation is given in the supplementary text. The estimated distance was approximately 40 nm, and it is undoubtedly smaller than the RTIL thickness of ca. 1 μm; that is, the polymerization reaction theoretically proceeds only at the vicinity of the RTIL surface.

In conclusion, the combination of the polymerizable [AllylEtIm][Tf₂N] and the FIB irradiation with a raster scanning mode enabled the preparation of micro/nanoscale 3D polymer structures. The interesting feature is that another polymer structure can be deposited on the top of the premade polymer deposit with ease as the 3D printers, which are rapidly becoming popular in several fields. Even the intricate polymer structure with hanging and bridging parts was produced at the resolution of approximately 100 nm. Thus, the RTIL-based FIB irradiation method reported in this article will make a large contribution to further development of the MEMS/NEMS technology and will make the 3D polymer micro/nanostructure fabrication closer to many scientists and engineers.

Methods

1-Allyl-3-ethylimidazolium bis((trifluoromethane)sulfonyl)amide ([AllylEtIm][Tf₂N]) was purchased from Kanto Chemical Co., Inc. 1-Vinyl-3-butylimidazolium bis((trifluoromethane)sulfonyl)amide ([VinylBuIm][Tf₂N]) was synthesized by the previously reported method^{42,43}. An n-Si wafer (100 Ω cm⁻²) purchased from Osaka Titanium Technologies Co., Ltd. was used as a substrate, and

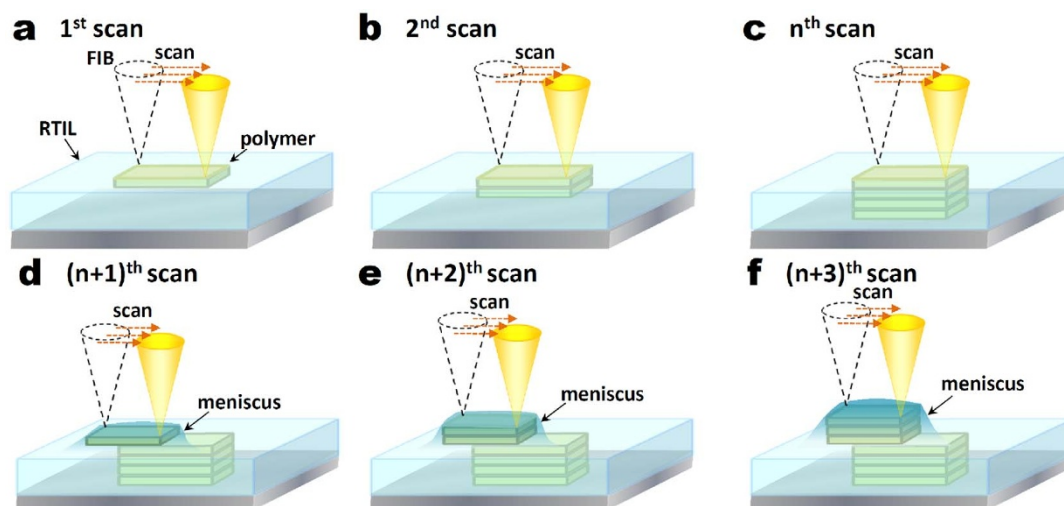


Figure 8 | Schematic illustrations of a plausible three-dimensional polymer structure formation process by RTIL-based FIB irradiation method. (a) At the initial stage, polymerization reaction proceeds by FIB irradiation at the surface of the polymerizable RTIL, [AllylEtIm][Tf₂N], and a polymer layer is formed. (b) The deposit grows downward until it reaches the Si substrate, when the FIB drawings are repeated. (c) After the deposit reached the Si wafer, it physically adheres to the substrate. (d–f) Once the structure is immobilized onto the Si wafer, subsequent FIB irradiation causes further polymerization on the immobilized structure due to the surface tension with meniscus of the RTIL. Finally, a three-dimensional polymer structure is produced by RTIL-based FIB irradiation method with a raster scanning mode.



the Si surface was coated with (3-aminopropyl)triethoxysilane⁴⁴ to improve its affinity to the RTILs. The resulting Si wafer was cut into $1 \times 1 \text{ cm}^2$ pieces. The RTIL diluted with ethanol to a concentration of ca. 5 vol% was spread onto the Si wafer to form a very thin and uniform RTIL layer on the Si wafer. After an appropriate amount of the RTIL ethanolic solution was dropped onto the Si wafer, it was spread by rotation at 4,000 rpm for 5 min. This spin coating technique resulted in a RTIL layer having a thickness of ca. 1 μm , which was confirmed by a confocal laser microscope (VK-8550, Keyence).

The RTIL-coated Si wafer was placed in a focused-ion-beam (FIB) instrument (SMI 2050, Seiko Instruments). A gallium ion beam accelerated at 30 kV was used to irradiate the Si wafer substrate. The ion beam currents and the beam size employed in this study were 210 pA and 23 nm ϕ , respectively. FIB drawing experiments were conducted by a common computer-aided FIB irradiation system using a bitmapped image prepared at a display frame of 800×800 pixels. The drawing of the images was performed in the raster scanning mode at a $40 \mu\text{m} \times 40 \mu\text{m}$ area. Consequently FIB was irradiated at a resolution of 500,000 dpi. After the FIB irradiation experiment, the Si wafer substrate was repeatedly immersed into an acetonitrile bath to remove unreacted RTIL and was dried in air. The fabricated figures were observed by a scanning electron microscope (VE-9800, Keyence) operated at an acceleration voltage of 20 kV with electron beam currents between 50 pA and 3.5 nA.

- Hill, A. R. Uses of Fine Focused Ion Beam with High Current Density. *Nature* **218**, 202–203 (1968).
- Kern, D., Kuech, T. & Oprysko, M. Future Beam-Controlled Processing Technologies for Microelectronics. *Science* **241**, 936–944 (1988).
- Gamo, K. Focused Ion Beam Technology. *Semicond. Sci. Technol.* **8**, 1118–1123 (1993).
- Chen, H. H. *et al.* Shocks in Ion Sputtering Sharpen Steep Surface Features. *Science* **310**, 294–297 (2005).
- Valentine, J. *et al.* Three-dimensional optical metamaterial with a negative refractive index. *Nature* **455**, 376–379 (2008).
- Getlawi, S., Koblichka, M., Hartmann, U., Richter, C. & Sulzbach, T. Patterning of permalloy thin films by means of electron-beam lithography and focused ion-beam milling. *Superlatt. Microstruct.* **44**, 699–704 (2008).
- Han, J., Lee, H., Min, B.-K. & Lee, S. J. Prediction of nanopattern topography using two-dimensional focused ion beam milling with beam irradiation intervals. *Microelectron. Eng.* **87**, 1–9 (2010).
- Matsui, S., Kaito, T., Fujita, J. & Komuro, M. Three-dimensional nanostructure fabrication by focused-ion-beam chemical vapor deposition. *J. Vac. Sci. Technol. B* **18**, 3181–3184 (2000).
- Hoshino, T. *et al.* Development of three-dimensional pattern-generating system for focused-ion-beam chemical-vapor deposition. *J. Vac. Sci. Technol. B* **21**, 2732–2736 (2003).
- Matsui, S. Focused-ion-beam deposition for 3-D nanostructure fabrication. *Nucl. Instrum. Methods Phys. Res., Sect. B* **257**, 758–764 (2007).
- Rogers, R. D. & Seddon, K. R. Chemistry. Ionic liquids--solvents of the future? *Science* **302**, 792–793 (2003).
- Endres, F., Bukowski, M., Hempelmann, R. & Natter, H. Electrodeposition of nanocrystalline metals and alloys from ionic liquids. *Angew. Chem. Int. Ed.* **42**, 3428–3430 (2003).
- Earle, M. J. *et al.* The distillation and volatility of ionic liquids. *Nature* **439**, 831–834 (2006).
- Armand, M., Endres, F., MacFarlane, D. R., Ohno, H. & Scrosati, B. Ionic-liquid materials for the electrochemical challenges of the future. *Nat. Mater.* **8**, 621–629 (2009).
- Huang, J. Y. *et al.* In situ observation of the electrochemical lithiation of a single SnO₂ nanowire electrode. *Science* **330**, 1515–1520 (2010).
- Wang, C. M. *et al.* In Situ Transmission Electron Microscopy Observation of Microstructure and Phase Evolution in a SnO₂ Nanowire during Lithium Intercalation. *Nano Lett.* **11**, 1874–1880 (2011).
- Wang, C. M. *et al.* In situ transmission electron microscopy and spectroscopy studies of interfaces in Li ion batteries: Challenges and opportunities. *J. Mater. Res.* **25**, 1541–1547 (2011).
- Vollmer, C. & Janiak, C. Naked metal nanoparticles from metal carbonyls in ionic liquids: Easy synthesis and stabilization. *Coord. Chem. Rev.* **255**, 2039–2057 (2011).
- Torimoto, T., Tsuda, T., Okazaki, K. & Kuwabata, S. New frontiers in materials science opened by ionic liquids. *Adv. Mater.* **22**, 1196–1221 (2010).
- Lovelock, K. R. J., Villar-Garcia, I. J., Maier, F., Steinrück, H.-P. & Licence, P. Photoelectron Spectroscopy of Ionic Liquid-Based Interfaces. *Chem. Rev.* **110**, 5158–5190 (2010).
- Villar-Garcia, I. J. *et al.* Charging of ionic liquid surfaces under X-ray irradiation: the measurement of absolute binding energies by XPS. *Phys. Chem. Chem. Phys.* **13**, 2797–2808 (2011).
- Kuwabata, S., Tsuda, T. & Torimoto, T. Room-Temperature Ionic Liquid. A New Medium for Material Production and Analyses under Vacuum Conditions. *J. Phys. Chem. Lett.* **1**, 3177–3188 (2010).
- Torimoto, T. *et al.* Sputter deposition onto ionic liquids: Simple and clean synthesis of highly dispersed ultrafine metal nanoparticles. *Appl. Phys. Lett.* **89**, 243117 (2006).
- Yoshii, K. *et al.* Platinum nanoparticle immobilization onto carbon nanotubes using Pt-sputtered room-temperature ionic liquid. *RSC Adv.* **2**, 8262–8264 (2012).
- Kuwabata, S., Kongkanand, A., Oyamatsu, D. & Torimoto, T. Observation of Ionic Liquid by Scanning Electron Microscope. *Chem. Lett.* **35**, 600–601 (2006).
- Arimoto, S., Oyamatsu, D., Torimoto, T. & Kuwabata, S. Development of in situ electrochemical scanning electron microscopy with ionic liquids as electrolytes. *ChemPhysChem* **9**, 763–767 (2008).
- Arimoto, S., Sugimura, M., Kageyama, H., Torimoto, T. & Kuwabata, S. Development of new techniques for scanning electron microscope observation using ionic liquid. *Electrochim. Acta* **53**, 6228–6234 (2008).
- Tsuda, T. *et al.* SEM observation of wet biological specimens pretreated with room-temperature ionic liquid. *ChemBioChem* **12**, 2547–2550 (2011).
- Uematsu, T., Han, J.-T., Tsuda, T. & Kuwabata, S. Metal-Ion Diffusion in Ionic Liquid Studied by Electrochemical Scanning Electron Microscopy with X-ray Fluorescence Spectrometry. *J. Phys. Chem. C* **116**, 20902–20907 (2012).
- Imanishi, A., Tamura, M. & Kuwabata, S. Formation of Au nanoparticles in an ionic liquid by electron beam irradiation. *Chem. Commun.* 1775–1777 (2009).
- Imanishi, A., Gonsui, S., Tsuda, T., Kuwabata, S. & Fukui, K. Size and shape of Au nanoparticles formed in ionic liquids by electron beam irradiation. *Phys. Chem. Chem. Phys.* **13**, 14823–14830 (2011).
- Talaty, E. R., Raja, S., Storhaug, V. J., Dölle, A. & Carper, W. R. Raman and Infrared Spectra and ab Initio Calculations of C₂-4 MIM Imidazolium Hexafluorophosphate Ionic Liquids. *J. Phys. Chem. B* **108**, 13177–13184 (2004).
- McMurry, J. *Organic Chemistry*. p. 341 (Brooks/Cole, 2007).
- Laible, R. C. Allyl Polymerizations. *Chem. Rev.* **58**, 807–843 (1958).
- Kometani, R. & Ishihara, S. Nanoelectromechanical device fabrications by 3-D nanotechnology using focused-ion beams. *Sci. Technol. Adv. Mater.* **10**, 034501 (2009).
- Igaki, J. *et al.* Comparison of FIB-CVD and EB-CVD growth characteristics. *Microelectron. Eng.* **83**, 1225–1228 (2006).
- Chang, Z. & LaVerne, J. A. Hydrogen Production in the Heavy Ion Radiolysis of Polymers. 1. Polyethylene, Polypropylene, Poly(methyl methacrylate), and Polystyrene. *J. Phys. Chem. B* **104**, 10557–10562 (2000).
- Tsukuda, S., Seki, S., Sugimoto, M. & Tagawa, S. Formation of Nanowires Based on π -Conjugated Polymers by High-Energy Ion Beam Irradiation. *Jpn. J. Appl. Phys.* **44**, 5839–5842 (2005).
- Tsukuda, S., Seki, S., Sugimoto, M. & Tagawa, S. Nanowires with controlled sizes formed by single ion track reactions in polymers. *Surf. Coat. Technol.* **201**, 8526–8530 (2007).
- Tagawa, S. *et al.* Ion beam induced nano-space reactions and nano-wire formation in polymers by high energy sub- μm heavy ion beams. *Surf. Coat. Technol.* **201**, 8495–8498 (2007).
- Ziegler, J. F., Ziegler, M. D. & Biersack, J. P. SRIM – The stopping and range of ions in matter (2010). *Nucl. Instrum. Methods Phys. Res., Sect. B* **268**, 1818–1823 (2010).
- Amajjahe, S. & Ritter, H. Anion Complexation of Vinylimidazolium Salts and Its Influence on Polymerization. *Macromolecules* **41**, 716–718 (2008).
- Green, M. D. *et al.* Alkyl-Substituted N-Vinylimidazolium Polymerized Ionic Liquids: Thermal Properties and Ionic Conductivities. *Macromol. Chem. Phys.* **212**, 2522–2528 (2011).
- Petri, D. F. S., Wenz, G., Schunk, P. & Schimmel, T. An Improved Method for the Assembly of Amino-Terminated Monolayers on SiO₂ and the Vapor Deposition of Gold Layers. *Langmuir* **15**, 4520–4523 (1999).

Acknowledgments

The authors would like to express their appreciation to A. Oshima of the Institute of Scientific and Industrial Research, Osaka University, for discussions and for performing the present experiments. The authors also thank R. Hagiwara and T. Nohira of the Graduate School of Energy Science, Kyoto University for measuring the micro-Raman spectra shown in Fig. 3. This study was supported by the Core Research for Evolution Science and Technology (CREST) from the Japan Science and Technology Agency (JST).

Author contributions

S.K., T.T., A.I. and T.T. designed the research; H.M. and K.I. prepared the samples and performed experiments; H.M., K.L., K.H., H.U., S.S. analyzed and interpreted the results; H.M. and S.K. developed the model; and S.K., H.M. and T.T. prepared this manuscript.

Additional information

Supplementary information accompanies this paper at <http://www.nature.com/scientificreports>

Competing financial interests: The authors declare no competing financial interests.

How to cite this article: Kuwabata, S. *et al.* Three-dimensional micro/nano-scale structure fabricated by combination of non-volatile polymerizable RTIL and FIB irradiation. *Sci. Rep.* **4**, 3722; DOI:10.1038/srep03722 (2014).



This work is licensed under a Creative Commons Attribution-NonCommercial-NoDerivs 3.0 Unported license. To view a copy of this license, visit <http://creativecommons.org/licenses/by-nc-nd/3.0>